A Digitally Controlled Drive System for Travelling-wave Ultrasonic Motor

GÜNGÖR BAL

A Digitally Controlled Drive System for Travelling-wave Ultrasonic Motor

Güngör BAL

Gazi University, Faculty of Technical Education, Department of Electrical Education,
06500 Ankara-TURKEY
e-mail: gunbal@gazi.edu.tr

Abstract

A digitally controlled drive system was implemented in this study to control the speed and direction of a travelling-wave ultrasonic motor. The drive system, based on a 2-phase voltage-fed high-frequency serial-resonant inverter, uses the mechanical resonant frequency of an ultrasonic motor. A TMS320F243 digital signal processor was used to control an ultrasonic motor drive system. The speed control of the ultrasonic motor was achieved with a driving frequency in the 41.3-43.3 kHz frequency range. The feasible evaluations of the proposed drive and control system were tested by experiments. Experimental results demonstrated that the proposed drive and control system is flexible and highly effective for the speed and direction control of a travelling-wave ultrasonic motor.

Key Words: *Ultrasonic motor, digital control, speed control, digital signal processor.*

1. Introduction

An ultrasonic motor (USM) is a new actuator that uses mechanical vibrations in the ultrasonic range as its drive source. USMs have important features such as high stall and specific torque, high torque at low speed, compactness in size, quiet operation and no electromagnetic interference [1-2]. The torque of an USM is 10 to 100 times larger than conventional electromagnetic motors of the same size or weight. Due to these features USMs are presently being used for industrial, medical, robotic, space and automotive applications [3].

Besides these advantages, USMs have some disadvantages that must be solved for practical applications. It is difficult to derive a complete mathematical model of USMs. Moreover, the control characteristics of USMs are complicated and highly non-linear. The precise values of motor parameters can not be obtained easily and the motor parameters are time-varying due to increases in temperature and changes in motor drive operating conditions such as driving frequency, source voltage and load torque [4-5]. In order to cope with these limitations of USMs several drive and control systems have already been proposed [6-9]. However, fluctuations in the speed tracking characteristics, especially under different speed and direction and varying load conditions, have not yet been sufficiently investigated from an experimental point of view.

The aim of the present study is to propose a highly effective drive system and obtain precise speed control characteristics for a travelling-wave USM (TWUSM). First, an equivalent circuit model of an USM is given. Then a digitally controllable driving system for the Shinsei's travelling-wave type USR60 USM is developed. To achieve precise speed control a TMS320F243 fixed point digital signal processor (DSP) was integrated into the USM drive system. All of the control signals were controlled by the DSP. The transient responses and steady state performances of the TWUSM have been obtained. The experimental results showed that the proposed digital drive and control system outputs robust, precise and rapid responses against the changes in speed and load conditions.

2. Travelling-Wave Ultrasonic Motor

Although several USM types have been designed, the rotary TWUSM is the most commonly used USM type. The TWUSM is driven by high frequency 2-phase sinusoidal voltages with a 90° phase difference. The speed of an USM is controlled by the amplitude, frequency and phase difference between the 2-phase voltages.

During the operation of USMs 2-stage energy conversion is formed. First, is the electro-mechanical energy conversion where the electrical energy is converted into mechanical energy. This is achieved by the excitation of piezoelectric ceramic with ultrasonic range frequency. Second, is the mechanical energy conversion where the mechanical vibrations are converted to linear or rotary motion by friction force generated in a stator-rotor interface [10-11].

The cutaway view of a Shinsei USR60 travelling-wave type USM used in the study is shown in Figure 1. The nameplate and parameters of this motor are given in the appendix. The USM mainly consists of stator and rotor components. The stator consists of the piezoelectric ceramic and the elastic body. The rotor is made from a bronze material pressed against the stator by means of a disc spring. When 2-phase voltages are applied to 2 orthogonal modes of piezoelectric ceramic of USM, elliptical waves occur on the stator surface. Then the rotor is driven by the tangential force at the contact surface resulting from the elliptical motion at the wave crests.
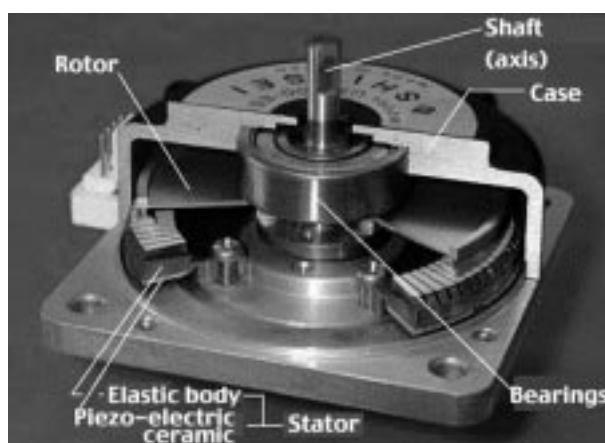

Figure 1. Cutaway view of Shinsei USR60 TWUSM.

The elliptical motion of points on the surface of the stator is generated by the travelling-wave in the stator. The vibrations are excited by a piezoelectric ceramic layer bonded to the lower surface of the stator. The rotor is driven by frictional forces in the contact layer. The rotation direction of the rotor is opposite to the direction of the travelling-wave.

To generate a travelling-wave within the stator, it is necessary to have control of 2 mechanical orthogonal modes. Electrode pattern A provides $cosk\theta$, and pattern B $sink\theta$. By driving these 2 modes 90° out of phase temporally a travelling-wave is produced. Patterns A and B provide a standing wave individually. The superposition of these standing waves produces a travelling-wave used in TWUSMs. By changing the sign of one of the drives signals the direction of the travelling-wave and thus the direction of the rotor changes [12].

The electrode arrangement in a disc-type piezoelectric ceramic is shown in Figure 2. The (+) and (-) symbols show the polarised directions. When a positive voltage is applied to a segment indicated by (+), it will expand. With a negative voltage it will contract. The reverse occurs for a (-) segment .
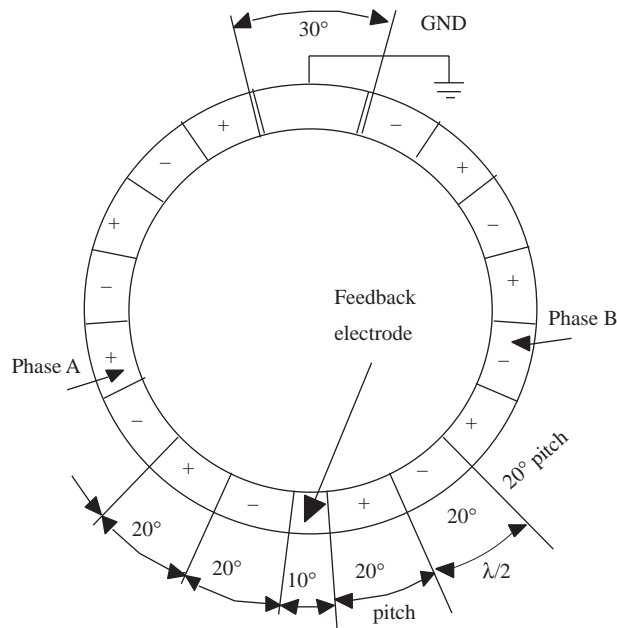

Figure 2. The piezoelectric disc and electrode arrangement of the USM.

The feedback electrode is mounted in addition to the A and B sections. This electrode produces high frequency AC voltage when mechanical vibrations act on the stator surface. The value of this voltage is proportional to the speed of the motor. To show the relation between the rotary speed and amplitude of feedback voltage, experimental measurements were made for different speed values. This relation is given in Figure 3. By using this relation, the speed control of the USM can be achieved without using an extra speed sensor.
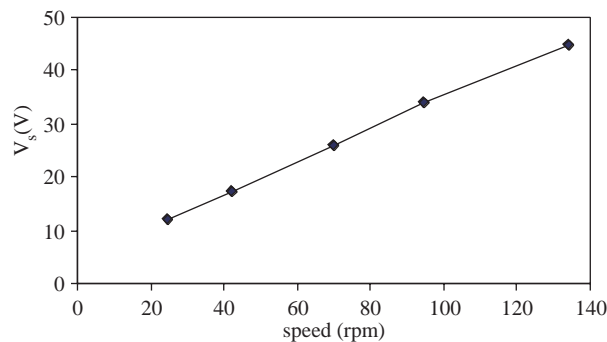

Figure 3. The relation between feedback voltage and speed.

To estimate motor parameters and characteristics an equivalent circuit representation of the USM is important. A single-phase equivalent circuit model of the USM is shown in Figure 4. Each phase of the USM is represented by damping capacitance C_d, which is due to the dielectric properties of piezoelectric ceramic. This capacitance is measured when the ceramic element is fixed so that no vibration can occur. In this condition there is no motion in the system. The damping capacitance of each phase of the USR60 USM was measured as to be 9 nF. r_d represents dielectric loss of piezoelectric ceramic. The combination of C_d and r_d is called the damping impedance. r_d can be ignored for the frequency range of USMs. C_m is the equivalent capacitor representing the spring effect of stator assembly, L_m is the equivalent inductor representing the mass effect of stator assembly. In the piezoelectric effect, a polarized element creates a hysteresis loop which results in losses. Furthermore, mechanical losses occur between metal and piezoelectric ceramic. These losses are represented by r_0 in the equivalent circuit. This component is also known as an internal resistor. The impedance combination of C_m, L_m and r_0 is called motional impedance.
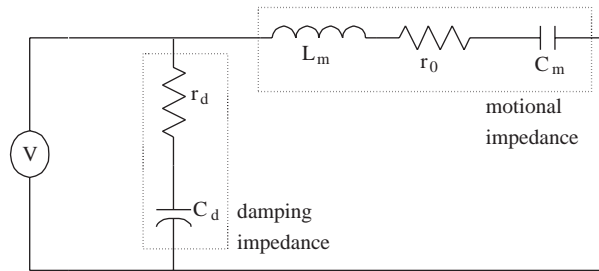

Figure 4. Equivalent circuit representation of the USM.

$C_m = A^2/s$ and $L_m = m/A^2$, where s spring constant of stator, m mass of metal assembly and ceramic of stator, A is force factor. The force factor is generally determined by the dimensions and material properties, also by the properties of the metal plate combined with it.

To provide high efficiency in the USM drive system, the USM should be driven at the near frequency creating resonance between C_m and L_m in the equivalent circuit. The mechanical resonance frequency is expressed as

$$f_m = \frac{1}{2\pi\sqrt{L_m C_m}} = \frac{1}{2\pi\sqrt{m/s}} \tag{1}$$

Damping admittance Y_d and motional admittance Y_m of the equivalent circuit are found as follows:

$$Y_d = \frac{1}{r_d + 1/j\omega C_d} \tag{2}$$

$$Y_m = \frac{1}{(r_0 + j\omega L_m + 1/j\omega C_m)} \tag{3}$$

$$Y_m = \frac{r_0}{r_0^2 + (\omega L_m - 1/\omega C_m)^2} + j\frac{1/\omega C_m - \omega L m}{r_0^2 + (\omega L_m - 1/\omega C_m)^2} \tag{4}$$

The sinusoidal current flowing into the motional branch causes motor movement called motional current, which is expressed by

$$I_m = V \times Y_m \qquad (5)$$

As before mentioned the speed of USM is controlled by the amplitude, frequency and phase difference of 2-phase voltages. Since the variable driving frequency method gives a more flexible control range than the other methods, in the present study the speed of the USM was controlled by variable driving frequency. Figure 5a shows a well-known speed-frequency characteristic of the USM. This characteristic was obtained by numerically solving the equivalent circuit model of the USM [13]. In the actual control of the USM, this characteristic was defined as a look-up table in the DSP. As seen from the Figure 5 this characteristic is not linear. In this study, motor speed was controlled at 41.3 kHz-43.3 kHz, which can be considered as the linear frequency range. Theoretical estimations were obtained from a steady-state model of the USM and these results were compared with experimental results. A sample result is given in Figure 5b to show the similarities between the estimation and experimental results. The detailed simulation results and validation of the model can be found in [13,14].
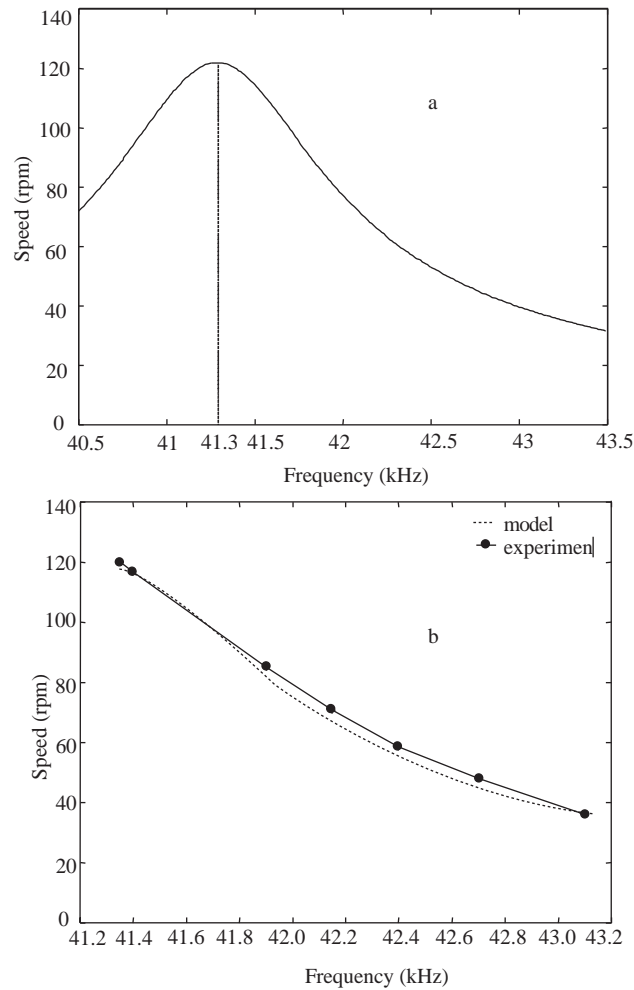

Figure 5. a) Speed-frequency characteristic of USM. b) similarities between results of the model and experiment.

3. Digital Controlled USM Drive System

For the practical operation of an USM a specific and well-defined power supply and high-quality semiconductor devices that can follow the optimum operating point of the motor are required. It is difficult driving piezoelectric ceramic owing to high damping capacitance. To easily drive the piezoelectric ceramic of USMs, the resonant frequency approach is preferred. For this reason a serial or parallel inductance is connected with each phase of an USM to provide resonant frequency. Figure 6 shows a newly developed drive system of a 2-phase high-frequency voltage fed serial-resonant inverter of the USM. This inverter includes pulse width modulation (PWM), pulse frequency modulation (PFM) and hybrid (PWM/PFM) control techniques. L_A and L_B inductances are connected in series with each phase to become resonant with the damping capacitance (C_d) of USMs. Inverter outputs are 2-phase high frequency AC voltages with 90° phase difference. The rotating direction is controlled by letting V_A or V_B lead. CW and CCW inputs provide direction control signals. In practice, the driving frequency is set higher than the resonant frequency of the mechanical vibration system due to basic operating characteristics of USMs [15,16].

The speed control of USMs was achieved by variable driving frequency. The value of the driving frequency was determined by comparing the AC voltage of feedback electrode (Vs) of the USM and a reference DC voltage (Vdc). The produced signal was then applied to the opto-isolator, split-phase and voltage control oscillator circuits.
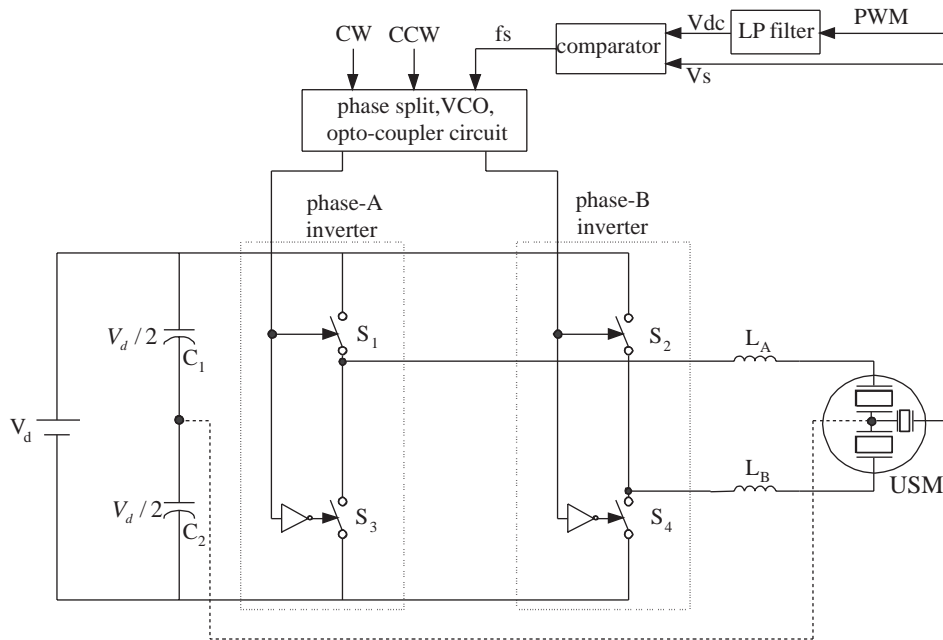

Figure 6. Drive system of the USM.

To provide sinusoidal output voltages, the input signal of S_1 was inverted and applied to S_3, and the input signal of S_2 was inverted and applied to S_4. The sequence of gate signals of inverter is given in Figure 7. By using this switching technique 2-phase output voltages with 90° phase difference were obtained.
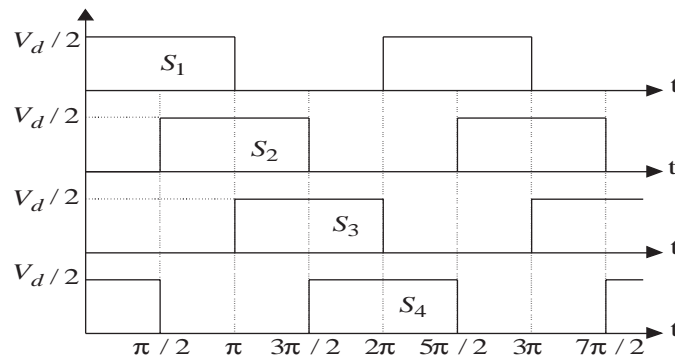
Figure 7. Switching sequence of inverter switches.

The control input of the drive system is switching frequency f_s. This input was obtained from a comparison of feedback electrode voltage (Vs) and reference DC voltage. According to the speed demanded, the value of the switching frequency was adjusted. This was achieved by changing the level of reference DC voltage. To change the level of DC voltage, the duty cycle of PWM signal was changed. So according to the duty ratio of PWM signal, the DC output of low-pass (LP) filter was controlled. The designed LP filter is shown in Figure 8. As seen from the figure, the input of the filter is a controllable PWM signal. According to the duty ratio of this signal, the filter produces DC voltage. When the duty ratio of the the PWM signal increases, the DC output value of the the filter increases.
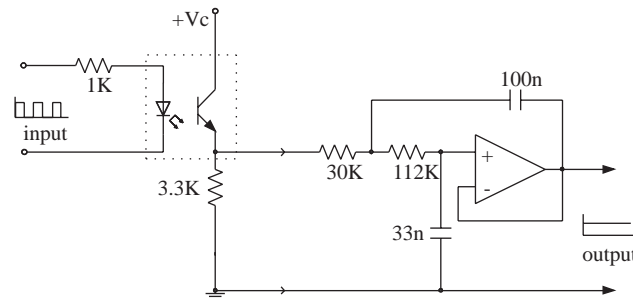

Figure 8. Designed low-pass filter.

For example; measured AC voltage of feedback electrode is shown in Figure 9. The value of this voltage is 34.6 V (rms) with 42.05 kHz frequency. To achieve the speed demanded, this voltage was compared with 2 V DC reference voltage as shown in Figure 10. By comparing these voltages a switching signal with $t = 2,394 \times 10^{-5}$ s ($f_s = 41,74$ kHz) was produced and this is given in Figure 11. Then, this switching signal was applied to 4 switches via voltage control oscillator and phase split circuits to provide 2-phase AC voltages. Figure 12 shows waveforms of these output voltages. As seen from the figure the frequency of voltages is 41.74 kHz, which is equal to switching signal frequency. The output voltages are equal and 120 V (rms). By changing the value of reference DC voltage the switching frequency f_s is changed and so the speed of motor is controlled.
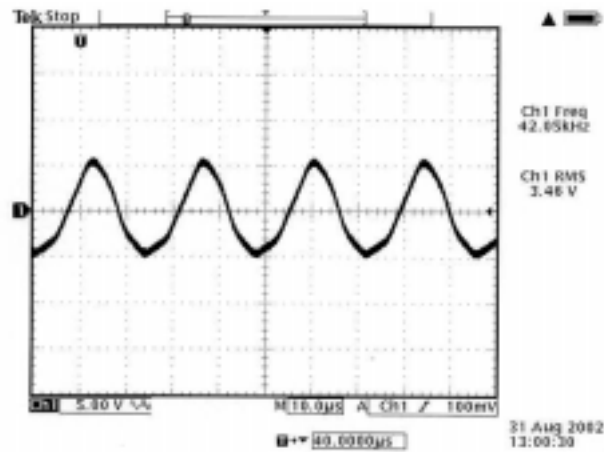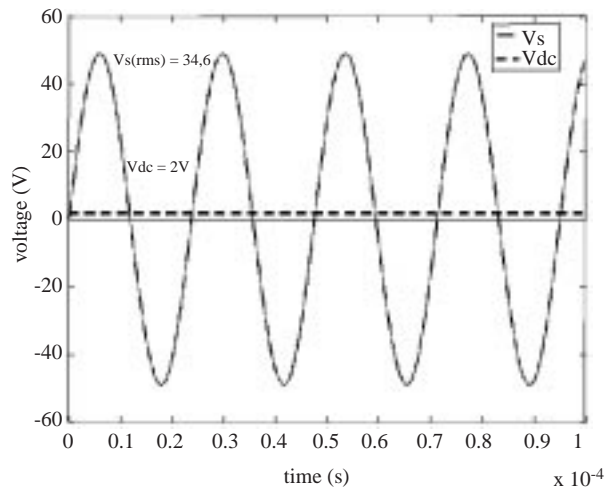
Figure 9. Voltage of feedback electrode.

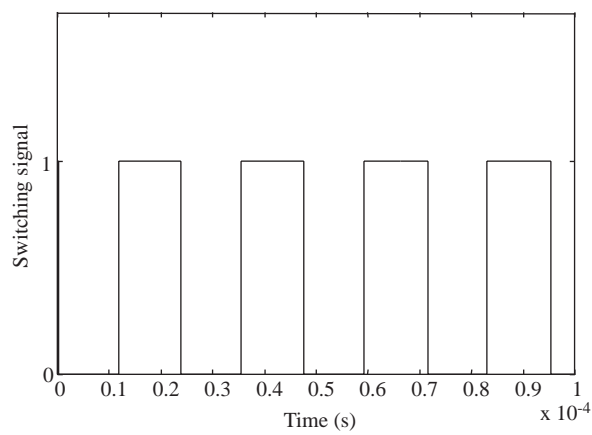**Figure 10.** Comparison of feedback voltage and reference DC voltage.

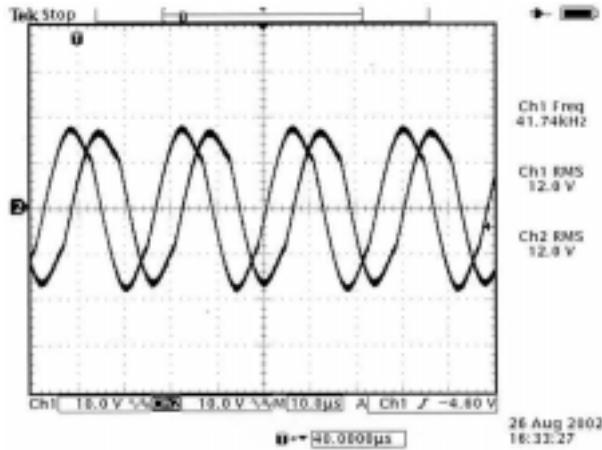
Figure 11. The switching signal.

Figure 12. Output voltages of inverter.

In the present study, an USM drive system was controlled by a 16-bit fixed point TMS320F243 EVM DSP. The block diagram of the TMS320F243-controlled USM drive system is given in Figure 13. The event manager and general purpose input/output (GPIO) units of DSP were used to control the USM. The PWM signal was generated by a general purpose timer-1 (GPT1), which was set in continuous-up count mode to provide asymmetric PWM signal. Two pins of GPIO were set as digital output to provide CW and CCW direction signals. The quadrature encoder pulse QEP circuit of the event manager was used for encoder signals. The encoder is 500-ppr and has 2 quadrature encoder signals and an index signal. These encoder signals were encoded digitally by QEP circuit and converted to the speed and position information for control purpose.
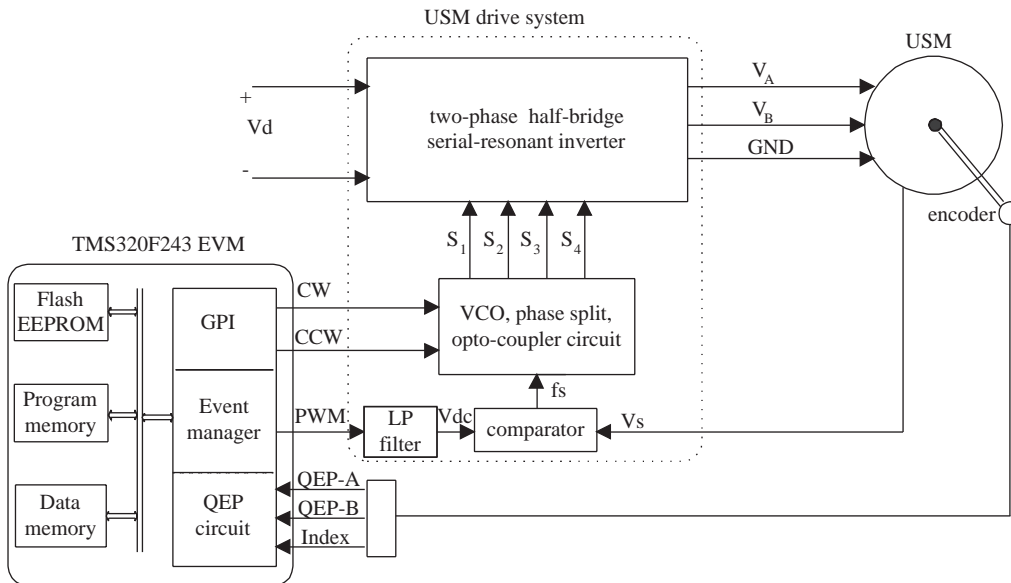

Figure 13. TMS320F243-controlled USM drive system.

The frequency of PWM signal is obtained as follows:

$$f = \frac{20\,MHz \times T1CON\_TPS}{P} \tag{6}$$

where 20 MHz is frequency of processor, P is period factor and *T1CON_TPS* is the 6-8 bits of general purpose timer control register (GPTCON). By adjusting the value of period factor P and *T1CON_TPS* bits the demanded frequency is obtained.

The main DSP control software can be divided into 2 parts. The first part is DSP initialization including register, core interrupt, peripheral, timers and subroutine initialization. These tasks are done once when the program starts. Following initialization, the program waits for interrupt calls while performing an infinite loop. The other part of the software is an interrupt service routine. This part includes the main software for USM control. This routine is called when a timer period occurs, as set in the initialization process. When an interrupt occurs, the main program breaks the infinite loop and goes into the proper interrupt service routine that has been designated for the particular event. The initialization and interrupt routines are shown as a flow diagram in Figure 14.
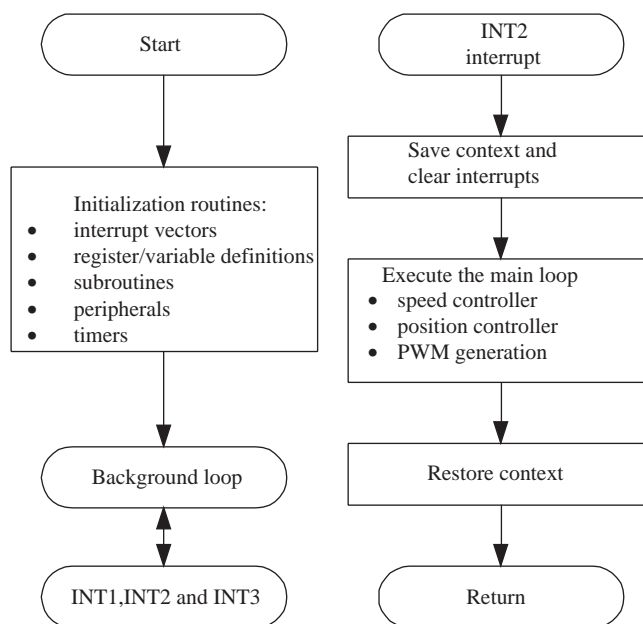

Figure 14. Flowchart of DSP program.

4. Experimental Results

In this section, the experimental results of a digitally controlled USM drive system are presented. The speed reference was obtained from output of low pass filter, which converts PWM signal as a reference DC voltage, and the actual speed was obtained from filtered voltage of a feedback electrode.

The developed drive system was designed to operate under different speed and load conditions. The step speed response of the USM was investigated for the unloaded and fully loaded conditions. While Figure 15a shows actual speed for un-loaded motor, Figure 15b shows actual speed for fully-loaded motor. From these figures it can be seen that the USM can operate smoothly without fluctuations under different load conditions.

When an up-down step reference speed is applied as shown in Figure 16a, the digitally controlled USM drive system can precisely and rapidly track the speed reference as shown in Figure 16b.
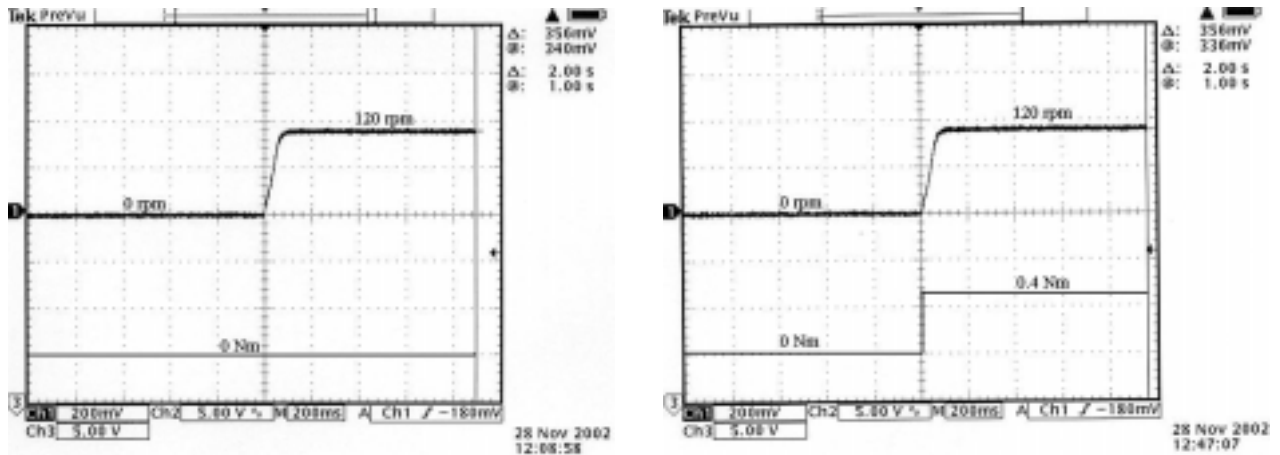
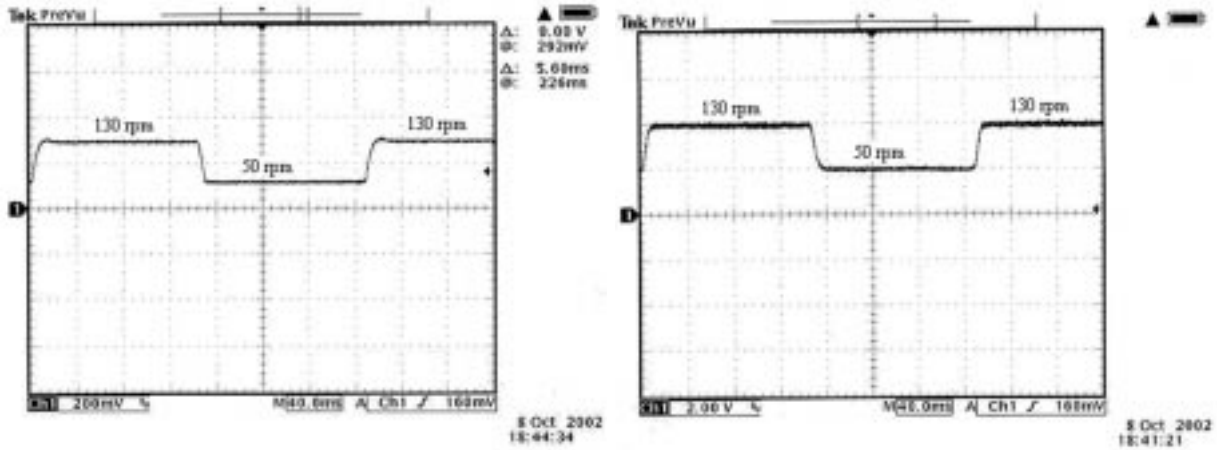**Figure 15.** Speed of USM (120rpm) a) No load b) 0.4 Nm load.

Figure 16. Up/down step reference speed a) reference speeds b) actual speed of USM.

To observe USM response time, Figure 16b is zoomed and given in Figure 17. As shown in the figure, the actual speed of the USM changes from 50 to 130 rpm in 6 ms.

In order to test the drive system under several speed changes, a speed reference as shown in Figure 18(a) is applied and the actual motor speed response is measured and given in Figure 18(b). As seen in the these figures, the USM tracks the references speed rapidly and precisely.

Besides the variable reference speed command if the rotor direction command of USM changes, the USM can track the reference speed and direction command. When the USM is normally running at 50 rpm in the CW direction, the speed command reverses to 100 rpm with the CCW direction. The speed command and quadrature encoder pulses are given together in Figure 19. To observe whether the motor follows the changes in speed and direction references Figure 19 is zoomed and given in Figure 20.

The incremental encoders provide 2-phase quadrature pulses with a $90°$ phase difference called phases A and B. With respect to the direction of rotation, the leading A and B phases change. According to these signals the change in direction of rotation can be observed. Figure 20 shows a point where encoder pulses change. From this point it is determined that the direction of rotation changes. The direction of rotation from CW to CCW is reversed in 6 ms, and the USM also reaches the new reference speed in CCW direction

in 6 ms. In other words, the USM can track the reference speed command from 50 rpm CW to 100 rpm CCW direction in 12 ms.
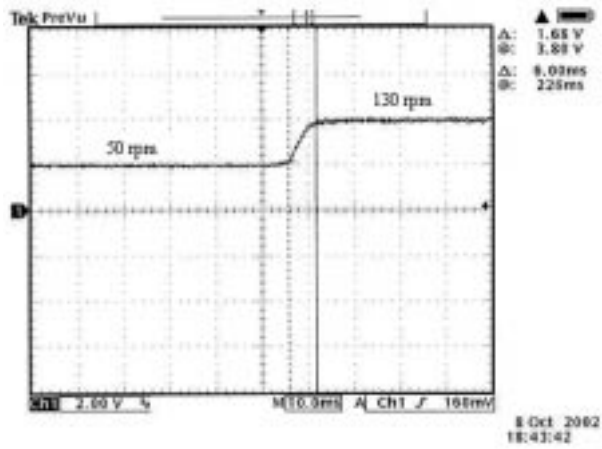

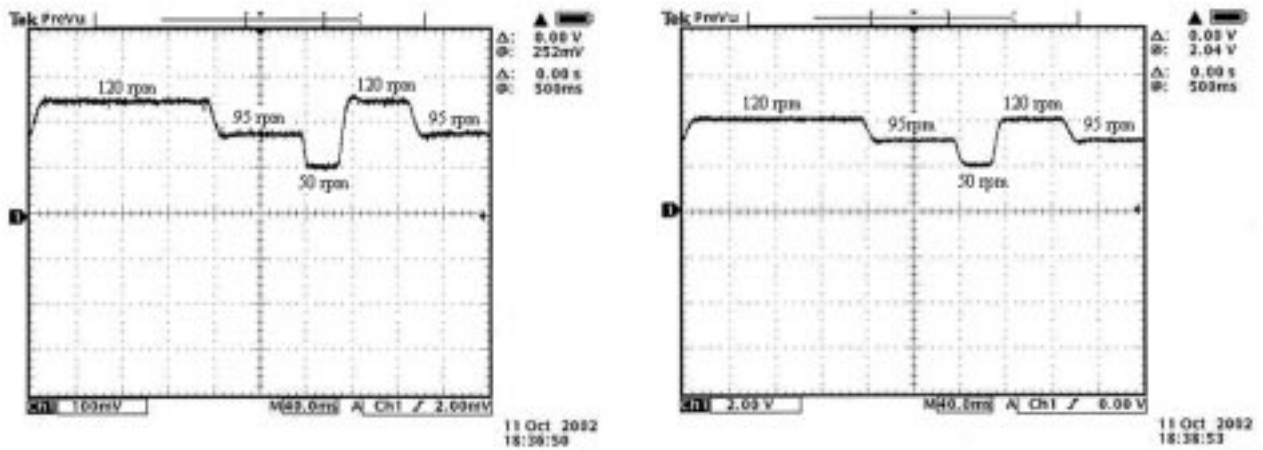**Figure 17.** Actual speed response time of USM (50-130 rpm).

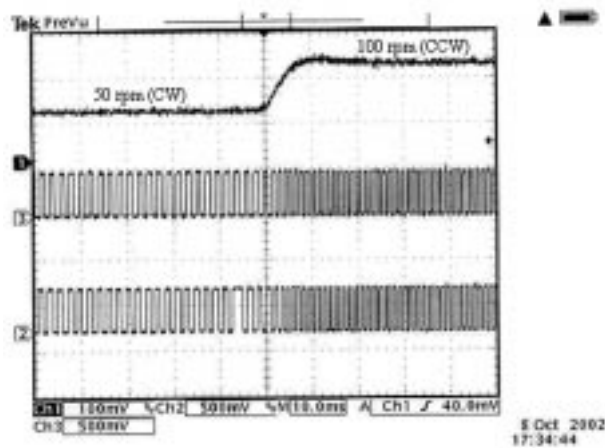**Figure 18.** Speed response of USM under changed command a) speed reference b) actual speed.

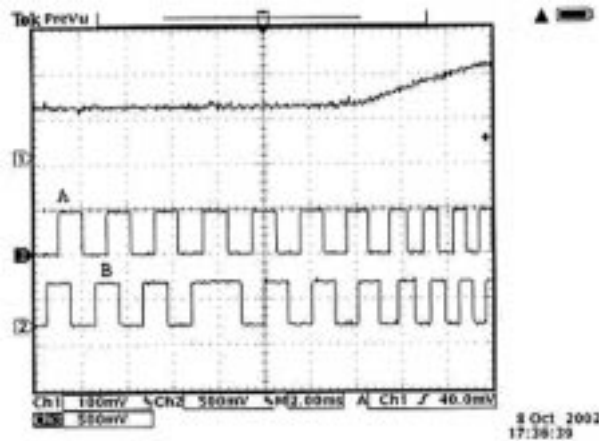**Figure 19.** Speed reference command with different rotation direction.

Figure 20. Zoom of Figure 19.

5. Conclusions

In this paper a digitally controlled drive system was implemented for a USR60 TWUSM. This control was achieved and optimised by TMS320F243 DSP. To drive the USM a high-frequency voltage-fed serial resonant inverter using the resonant technique was designed. The speed of the USM was controlled by driving frequency, which controls detecting resonant state by generated voltage of the feedback electrode mounted on the USM. This control system compensates for variations in the speed characteristics of the motor.

The performance of the proposed drive and control system was demonstrated with experimental results. The feasible effectiveness of the USM under transient and steady-state conditions was investigated. Experimental results show that the developed drive and control system gives superior speed characteristics for the USM under different load, direction and speed conditions. The proposed control scheme is new and very effective for a TWUSM.

References

[1] T. Sashida, T. Kenjo, An Introduction to Ultrasonic Motors, Oxford University Press, New York, 1993.

[2] K. Uchino, "Piezoelectric ultrasonic motors: Overview", Smart Material Structure, vol. 7, pp. 273-285, 1998

[3] K. Nakamura, S. Ueha, "Potential ability of ultrasonic motors: A discussion focused on the friction control mechanism", Electronics and Communications in Japan, Part 2, 81(4), pp. 57-67, 1998.

[4] H. Storck, J. Wallaschek, "Experimental investigations on modelling assumptions in the stator/rotor contact of travelling-wave ultrasonic motors", Journal of Vibroengineering, Vol. 4, 2000.

[5] F.J. Lin, R.J. Wai, C.M. Hong, "LLCC resonant inverter for piezoelectric ultrasonic motor drive", IEE Proc. Electr. Power Applications, Vol. 146(5), pp. 479-48, 1999.

[6] T. Senjyu, S. Yokoda, H. Miyazato, K. Uezato, Speed control of ultrasonic motors by adaptive control with simplified mathematical model, IEE Proc. Elect. Power Appl., Vol. 145(3), pp. 180-184, 1998.

[7] A. Ferreira, P. Minotti, "High-performance load-adaptive speed control for ultrasonic motors", Control Engineering Practice, Vol. 6, pp. 1-13, 1998.

[8] Y. Izuno, et al., Speed tracking servo control system incorporating travelling-wave type ultrasonic motor and feasible evaluations, "IEEE Transactions on Industry Applications", Vol. 34 (1), 126-132, 1998.

[9] L. Petit, N. Rizet, R. Briot, P. Gonnard, "Frequency behavior and speed control of piezomotors", Sensors and Actuators A, Vol. 80, pp. 45-52, 2000.

[10] H. Storck, J. Wallaschek, "The effect of tangential elasticity of the contact layer between stator and rotor in travelling-wave ultrasonic motors", Int. J. Nonlinear Mechanics, Vol. 38, pp. 143-159, 2003.

[11] Y. Ming, Q. Peiwen, "Performances estimation of a rotary travelling-wave ultrasonic motor based on two-dimension analytical model", Ultrasonics, Vol. 39, pp. 115-120, 2001.

[12] N.W. Hagood, A.J. McFarland, "Modelling of a piezoelectric rotary ultrasonic motor", IEEE Transactions on Ultrasonic, Ferroelectrics and Frequency Control, Vol. 42 (2), pp. 210-224, 1995.

[13] G. Bal, E. Bekiroglu, "Characteristics estimation of travelling wave ultrasonic motors using equivalent circuit model", in Proc. Int. Conf. on Electrical and Electronics Eng. ELECO'2001, Bursa-Turkey, pp. 62-66, 2001.

[14] G. Bal "Fuzzy logic based speed/position control implementation of ultrasonic motor with DSP" TÜBİTAK Research Project Final Report, October 2002.

[15] S. Furuya, T. Maruhashi, Y. Izuno, Load-adaptive frequency tracking control implementation of two-phase resonant inverter for ultrasonic motor, IEEE Transactions on Power Electronics, Vol. 45(3), pp. 542- 550, 1992.

[16] F.J.Lin, R.Y. Duan, J.C. Yu, "An ultrasonic motor drive using a current-source parallel-resonant inverter with energy feedback", IEEE Transactions on Power Electronics, Vol. 14(1), pp. 31-42, 1999.

Appendix

The nameplate of USR60 USM

Drive frequency	40-44 kHz
Drive voltage	100-130 Vrms
Drive current	53mA
Rated torque	0.4 Nm
Rated power	4 W
Rated speed	10 rad/s
Holding torque	<=800mNm
Rotor inertia	7.2×10^{-6} kg/m^2
Weight	0.23 kg

The equivalent circuit parameters of USR60 USM

$C_d = 9$ nF
$r_d = 20$ kΩ
$L_m = 0.1$ H
$r_0 = 150$ Ω
$C_m = 168$ pF